

FATIGUE STRENGTHS OF DIAPHRAGM JOINT IN BOX-SECTION TRUSS CHORDS OF HIGH STRENGTH STEEL

By Koei TAKENA, Hirosuke SHIMOKAWA*, Fumio ITOH** and Chitoshi MIKI****

Large scale specimens of transverse fillet welded joints which were assembled using thicknesses and shapes similar to those of the actual structures, and the improved weld electrodes were tested. Specimens were cruciform welded joints, box-section and H-section members of 600 MPa, 800 MPa and 500 MPa class steels. Effects of stress ratios, weld toe profiles, scallops and single-side fillet welding of the end diaphragm on the fatigue strength of joints were examined.

Keyword : fatigue, fillet welds, high strength steel

1. INTRODUCTION

Until recently, quenched and tempered high strength steel has been used on limited occasions in railroad bridges where cyclic stresses are dominant in design stresses. In the long span bridges on the D-route of the Honshu-Shikoku bridge project, which involves highways and railroads, usage of a great amount of high strength steels, whose tensile strength is greater than 568 N/mm² (SM 58, HT 70 and HT 80), became necessary. Thus, many fatigue tests using small model specimens of high strength steels were carried out by the Honshu-Shikoku Bridge Authority in the 1970's¹⁾. From these results, the fatigue strength of the fillet welded cruciform joint of HT-80, which used the conventional, low hydrogen type welding electrode turned out to be somewhat lower than that obtained by the design life curve for category C joints in the steel railroad bridge design code²⁾.

In the fatigue design of truss chords, the fatigue strength of the transverse fillet welded joint for the attachment of a diaphragm often become a decisive factor. Therefore, various kinds of method such as grinding and peening have been tried to increase its fatigue strength. From these experimental grinding and peening have been tried to increase its fatigue strength. From these experimental results, it appears that usage of a specially designed welding electrodes (improved electrodes) for fillet welds, to obtain smooth toe profiles, is the most practical method³⁾.

In order to validate the applicability of the results which were obtained from fatigue tests on small specimens, fatigue tests were carried out on large scale specimens of transverse fillet welded joints which were assembled with a thickness and shape similar to the actual structure and using the improved weld

* Member of JSCE, Honshu-Shikoku Bridge Authority (Mori Bld., 22, Toranomon, Minato-ku, Tokyo 105)

** Member of JSCE, Japan Construction Method and Machinery Research Institute (Oobuchi, Fuji-city, Shizuoka 417)

*** Member of JSCE, Dr. Eng., Tokyo Institute of Technology (Ookayama, Meguro-ku, Tokyo 152)

electrode. The objectives of this study were to examine the effects of stress ratios, weld toe profiles of multi-layered fillet welds, scallops of the diaphragm, and single-side fillet welding of the end diaphragm on the fatigue strength of joints.

2. Experimental Methods

(1) Specimens

Configurations and sizes of specimens are shown in Fig.1. Mechanical properties and chemical compositions of tested steels are shown in Table 1. The welding procedure is shown in Table 2.

In specimens RA and RB (thickness of the plates : 45 mm and 75 mm, respectively), ribs are attached by double and triple layers manual welding, respectively, using an improved electrode, LBF²⁾, perpendicular to the rolling direction of the base plate of HT 80. Since the third layer of the RB specimen did not affect the fatigue strength, conventional low hydrogen type electrodes, LB 62, were used. In the three-layered welding, fillet welding of equal leg size was usually used for the first layer in order to provide deep penetration into the weld root. However, in the RB specimen, extremely unequal leg size fillet welding was used on the first layer to obtain smooth profiles of weld toe (Fig. 2).

The BA specimen had a box cross section consisting of a 15 mm thick HT 80 steel plate. Submerged arc welding was used for corner welding and a diaphragm was manually welded using the improved electrodes. In order to examine the dependence of fatigue strength upon a difference in the treatment of the stop and start of fillet welding used to attach a diaphragm (Fig. 2), two methods were used : (1) a method whereby scallops were placed and welding continuously encircled them (a method commonly used in bridges in Japan), and (2) stop and start welding of each side at each corner overlap.

The HC specimen was assembled using the welding method which was developed based on the above fatigue test results and which has been adopted for the fabrication of Honshu-Shikoku Bridges. The main material is SM 58, the welding electrode was LBF 52, and scallops were provided for the diaphragm. In order to reduce weld defects in the transverse fillet welds, welding was started by two

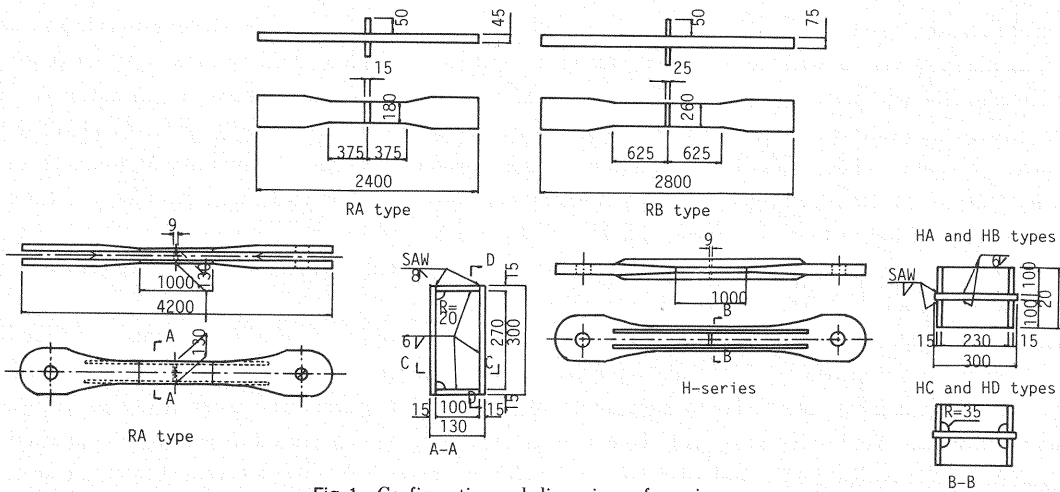


Fig. 1 Configuration and dimensions of specimens.

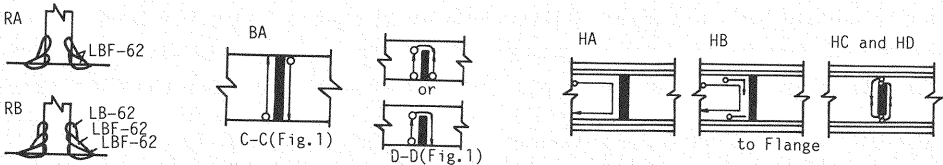


Fig. 2 Welding details and welding sequences.

Table 1 Mechanical Properties and Chemical Composition.

Specimen	Plate	Mechanical Properties			Chemical Composition											Remarks
		Yield Point	Tensile Strength	Elongation	C	Si	Mn	P	S	Ni	Cr	Mo	V	B	Cu	
		N/mm ²	N/mm ²	%	×100			×1000			×100			×1000		
RA	HT80, t=45	77	84	24	10	27	97	15	5	10	59	33		2		Main Plate
	HT80, t=15	79	83	29	12	29	92	12	7	10	55	40				Rib Plate
RB	HT80, t=75	82	88	24	12	31	90	12	6	13	58	40		2		Main Plate
	SM50, t=25	34	52	23	16	38	137	20	24							Rib Plate
BA	HT80, t=15	85	90	29	11	26	97	18	8	8	53	39	44	18	26	Main Plate
	SS41, t=9	31	46	31	16	19	66	20	9							Diaphragm
HA, HB	SM58Q, t=15, 20	66	72	35	16	29	136	19	9	7	5	50				Main Plate
	SS41, t=9	31	45	30	14	20	90	15	11							Diaphragm
HC	SM50Y, t=15, 20	42	56	25	17	38	142	19	8							Main Plate
	SS41, t=9	31	45	30	13	20	90	9	8							Diaphragm

Table 2 Welding Conditions.

Specimen	RA	RB	BA	HA		HB	HC	HD
				HA ₀	HA ₁			
Main Plate	HT80	HT80	HT80	SM58Q	SM58Q	SM58Q	SM58Q	SM50Y
Diaphragm	HT80	SM50	HT80	SS41	SS41	SS41	SS41	SS41
Root Gap (mm)	0	0	1	0	1	1	1	1
Electrode	LBF-62	LBF-62 LB-62	LBF-62	LBF-52A	LBF-52A	LBF-52A YM-26	LBF-52A	LBF-52A
Scallop	x	x	o	x	x	x	o	o

welders from a common welding pool near the central part of the thickness of the plate at the scallop. (Fig. 2). Since the end of the welding comes at the center of the diaphragm, a crater was left at that spot. For comparison with non-quenched steel, SM50Y was used for the HD specimen. The assembling procedure was the same as that of the HC specimen.

Only HA and HB specimens are fillet welded joints with a single side which simulates the end diaphragm of the truss chord. In the HA specimen, the main plate was made of SM58. As shown in Fig. 1 and 2, the diaphragm was a single side fillet welded with a LBF 52 electrode: the welding was conducted without interrupting the arc around corners and was continued to the vertical bead. To investigate the effect of the root gap, the root gaps of HA₀ and HA₁ specimens were set at 0 mm and 1 mm, respectively. In order to enable deep penetration of welding at corners, CO₂ semiautomatic welding was carried out from the point just before the corner to tack welds on the web, and then manual fillet welding was done in HB specimens. Other conditions of HB specimen were the same as for the HA specimen.

(2) Measurement of the profiles of weld toe

Silicon material with small shrinking was used to obtain the shape of the weld toe of the specimens. The toe radius, ρ and flank angle, θ , which are the major defining figures of the shape of weld toes, were measured by taking a slice of 0.5 mm of mold around the section, being checked. These were magnified 20 times and measured. Flank angle θ was defined as the angle between the main plate and the average line of the surface of the weld bead 10 mm from the weld toe. In actual measurements, bumps of less than 1 mm were ignored.

(3) Fatigue test

Fatigue tests were carried out by using a servo-controlled large fatigue test machine with a dynamic capacity of 4 MN. The loading rate was 180~480 rpm. The stress ratio R was set at -1 , 0 , and 0.6 for RA and at 0 for all other specimens. For the purpose of investigating the initiation and propagation behavior of fatigue cracks, beach marks were created on the failure surface for part of RA, BA, HA, HB and HC (beach mark test). The stress range was halved by increasing the minimum stress at certain numbers in beach mark test. The observation of beach marks was done by a microscope of 40 times magnification.

3. RESULTS OF THE FATIGUE TEST

(1) Fatigue strength

The fatigue test results are shown in Table 3. The repetitive number of cycles of halved stress range is

Table 3 Fatigue Test Results.

SPECIMEN	STRESS RANGE N/mm ²	FAILURE LIFE x10 ³ cycle	BEACH MARK TESTS		RE-TESTS		REMARKS
			STRESS	BLOCKS	STRESS RANGE N/mm ²	FAILURE LIFE x10 ³ cycles	
RA-1	130	3285					
RA-2	129	4000					R=0.6
RA-3	195	465					"
RA-4	270	393					"
RA-5	386	120					"
RA-6	147	1136	5	5			
RA-7	208	477					
RA-8	300	185					
RA-9	208	437					
RA-10	130	4000			149	1274	
RA-11	130	1573					
RA-12	130	3285			149	1817	
RB-1	131	3214					
RB-2	141	3242					
RB-3	197	386					
BA-1	159	890	7	7			
BA-2	133	1304	9	9			
BA-3	118	2785	15	15			
HAQ-1	103	3860	12	12			
HAQ-2	103	3429	11	11			
HA1-1	103	2670	9.2	9.2	134	450	
HA1-2	104	3230	10	10			
HA1-3	154	894	4	4			
HA1-4	131	1616	8	8			
HB-1	103	3312	11	11			
HB-2	103	2517	8	8			
HC-1	116	3006	7	7			
HC-2	131	1384	4	4			
HC-3	154	1091	5	5			
HD-1	160	1000	5	5			
HD-2	119	5100	17.2	2.2	177	542	
HD-3	134	1664	5	5			

run out

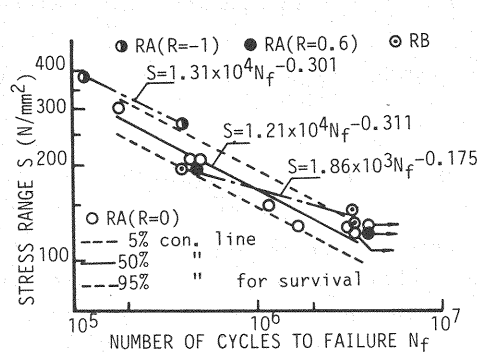


Fig.3 Fatigue Test Results of RA and RB specimen.

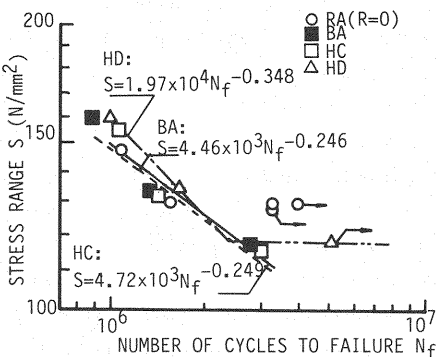


Fig.4 Fatigue Test Results of BA, HC and HD specimen.

not included in failure life. In Fig. 3 through 7, the relationships between stress range and failure life and the linear regression lines as obtained by the least square method are shown for each test series.

Fig. 3 shows the results for RA and RB specimens. The fatigue strength of large scale welded joints did not depend on the stress ratios due to the high tensile residual stress. However, the fatigue strengths of $R = -1$ are slightly higher when compared with those of $R = 0$ and $R = 0.6$ for the RA specimen. The experimental results obtained from specimen RB are scattered around the confidence lines of 5 % and 95 % for survival of RA specimens. These results suggest that the effect of plate thickness on the fatigue strength of this joint is not significant. As described in (2) the initiation points of fatigue cracks in RB specimens are always at the weld toe of the second layer and the shape of the weld toe varies with the performance of welding (Fig. 7). Therefore, these test data are not adequate for the quantitative evaluation of the effect of plate thickness on fatigue strength. These results indicated a difficulty in the quality control of uniform weld toe profiles in actual members, therefore, this welding method was abandoned in the fabrication of Honshu-Shikoku bridges.

In Fig. 4, the test results for specimens BA, HC, and HD, whose shapes are close to those of the actual structural members, are shown for comparison. This figure indicates that there is not much difference in fatigue strength between specimens BA and HC. In the stress range approximately 150 N/mm², there is

almost no difference in fatigue life between specimen HC of SM 58 steel and specimen HD of SM 50 Y steel. However, the difference is obvious at a stress range of approximately 120 N/mm². As shown in Table 3 and as discussed in (2), in HC-1 ($S_r=116$ N/mm²), a fatigue crack occurred before 400 000 cycles. Contrary to this, in HD-2 ($S_r=119$ N/mm²) a fatigue crack occurred only after 4 500 000 cycles of stress were applied. These results agree with the results of many previous studies that quenched type high strength steels have higher notch sensitivity to fatigue crack initiation compared to non-quenched type steels¹⁰ and the fatigue limits of welded joints of quenched type steels are often lower than those of non-quenched type steels.

When the fatigue lives of specimen HC and RA are compared, there is no difference at the stress range of approximately 150 N/mm². However, the fatigue strength of specimen HC, which has a similar joint shape of actual structure, showed obviously low fatigue resistance below approximately 120 N/mm². As described in (2), the flank angle and radius of weld toe near the scallop becomes steep and sharp compared with the middle part of the weld bead of HC. Most cracks start at these points. Thus, RA which was made similar to the middle section of the weld beads, has a smaller stress concentration compared to HC; in addition, there is high tensile residual stress at the corners of HC specimen. Considering that the stress range is important at this level and that actual welding of these points is generally conducted in bad conditions in places where not much working space is available. It may be concluded that fatigue phenomena of an actual structure cannot be reproduced in cruciform welded joints specimen such as RA type, which is a simplified and idealized specimen.

In the new fatigue design code⁶, the effect of average stress is considered to be none for the stress ratio $R > -1$. In Fig. 5, the results of large scale fatigue tests for the stress ratio $R > -1$ (including the results of cruciform joints with scallop⁵), 5 % and 95 % confidence lines for survival, and a new design life curve for category C joints are shown. The results for specimens BA and RB were neglected because their welding was conducted by the method which was rejected for use in the Honshu-Shikoku bridges. The 95 % survival line from the test results agree very well with the design curve.

Fig. 6 shows 5 %, 50 %, and 95 % confidence lines for survival from the test results with small test specimens which were welded using conventional low hydrogen welding electrodes; results of the above mentioned large scale fatigue tests are also shown. It is pointed out that fatigue strength decreases as plate thickness increases, and this concept was adopted in some design standards^{6,7}. However, in the large scale specimens built using improved electrodes, fatigue strength increased considerably compared

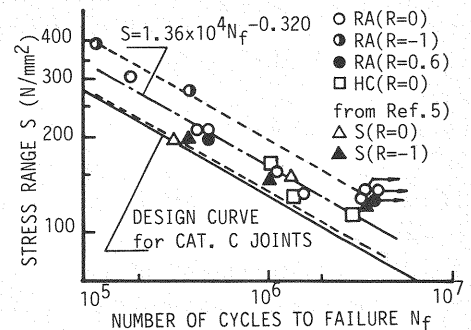


Fig. 5 Fatigue Test Results of Stress Ratio $R \geq -1$

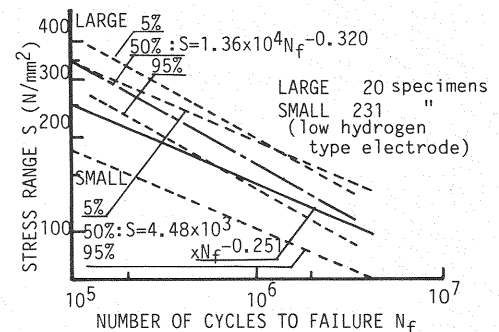


Fig. 6 Fatigue Test Results of Large and Small Specimen.

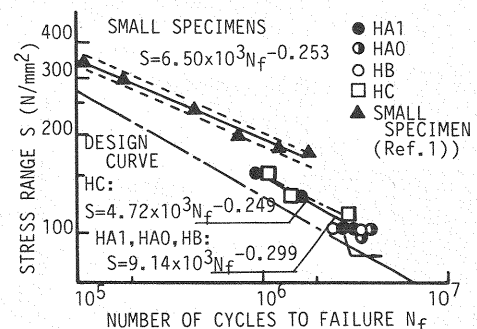


Fig. 7 Fatigue Test Results of Single Fillet Welded Joints.

with the small scale specimens of conventional electrodes.

Fig. 7 shows the fatigue test results of large scale single-sided fillet welded diaphragm joint specimens, small scale single-sided fillet welded specimens and the design curve for C class joints. There was not much difference in the fatigue strength among specimens HA₀, HA₁, and HB whose welding method was altered. Furthermore, when compared with the performance of specimen HC, in which both sides of the diaphragm plate were welded, there was not much difference in fatigue strength. The fatigue strength of small specimens is far higher than that of large scale specimens. This can be explained because, as seen in the cross rib in single side fillet weld joints, as the concentration of stress on joints increases, the conditions of various factors which affect fatigue, such as residual weld stress and defects, will vary greatly between the actual structures and a small scale specimen.

(2) Initiation and propagation of fatigue cracks

As shown in Table 3, the numbers of applications of “half loading” and the numbers of beach marks agreed in all specimens which underwent the beachmark test except for the ones which were retested. This indicates that the fatigue cracks initiated and started to propagate at the beginning of stress repetition. It also indicates that major part of the fatigue failure life is consist of the life required in the propagation of cracks.

The radius ρ and flank angle θ of the weld toe at crack initiating points in RA and RB specimens are shown in Fig. 8 ; examples of their shapes are shown in Fig. 9. In RA, the majority of fatigue cracks started at the weld toe in the first welding layer. In RB-type specimens an increase in the flank angle in the first layer was expected to improve fatigue strength. However, all specimens failed due to the cracks which started at the weld toe of the second layer. This can be explained because although the nominal stress at the terminal point in the second layer was only reduced by approximately 3 %, the shape deteriorated considerably in comparison with that of the first layer. As shown in Fig. 8, the flank angle of RB became

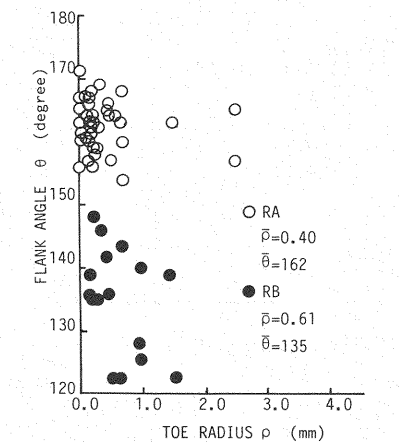


Fig.8 Flank Angle and Radius at Weld Toe.

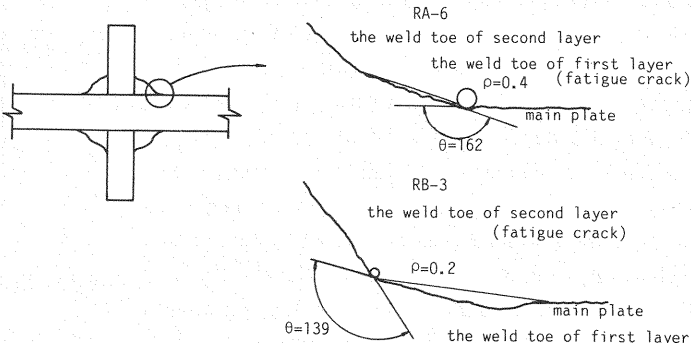


Fig.9 Weld Toes of Fillet Welded Joint RA and RB.

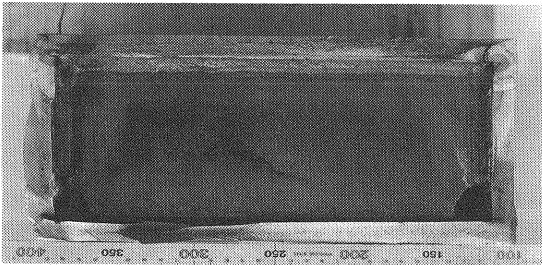
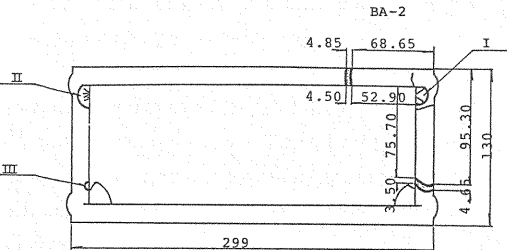


Photo 1 Failure surface of BA-2 specimen.



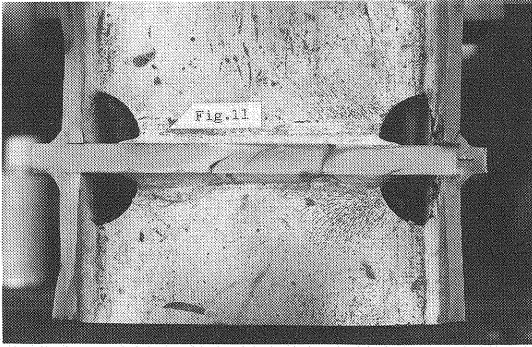


Photo5 Failure surface of HD-2 specimen.

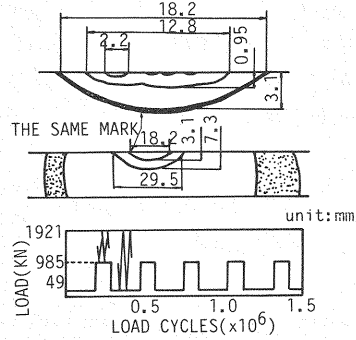


Fig.11 Beach Marks on the failure surface of HD-2 specimen.

Photo 4, a crack developed from a crater in the midsection of a diaphragm. Thus, if the shape of the terminals deteriorates, fatigue strength decreases even if this occurs in the midsection. Photo 5 and Fig. 11 show specimen HD-2 which was forced to fail during a retest by repetition at a higher stress range ; this followed the original fatigue test. The first fatigue test was conducted at $S_r=119\text{ N/mm}^2$ and the number of half loading blocks was 17. In the retest, stress range was set at 177 N/mm^2 and the corresponding half loading blocks were two. Four beachmarks are observed on the failure surface. The first two were produced by the first series of load repetition and shows that these cracks initiated after 4 500 000, cycles of repeated loading.

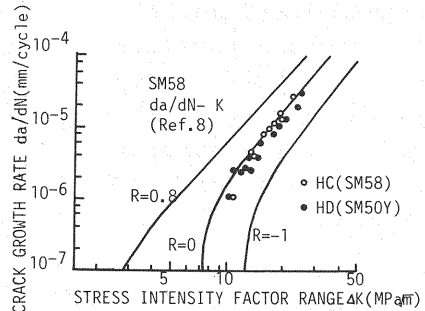
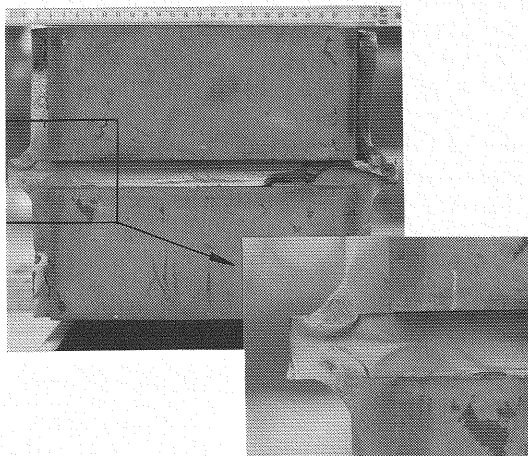
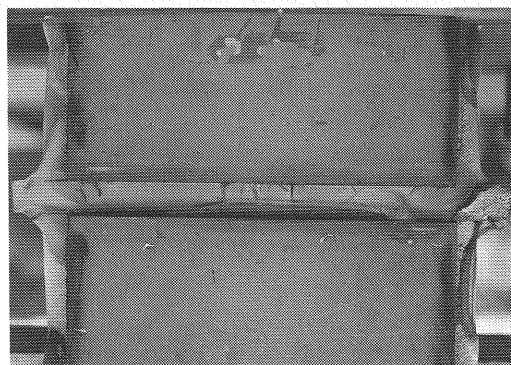


Fig. 12 Fatigue Crack Propagation rate.

In Fig. 12 the relationship between the ranges of stress intensity factor and crack propagation rates which were obtained from the spacings of beach marks on the failure surfaces of HC and HD specimen are demonstrated. Computational results by Maddox et al.⁹⁾ were used to calculate the range of the stress intensity factor of corresponding fatigue cracks. As shown in Fig. 12 the fatigue crack propagation rate in HC specimens of quenched type high tensile steel and in HD specimens of non-quenched type steel are almost equal. Hence, the difference in fatigue is found in the low stress range (approximately 120 N/mm^2) and can be considered to be due to variation in the number of occurrences of fatigue crack initiation (N_c).

In specimens HA and HB, which were built by single-sided fillet weld, all failures occurred by fatigue cracks originating at the root of the weld. No cracks were detected at the fillet weld toe by magnetic particle examination. As can be observed in Photo 6, many fatigue cracks of semielliptical and quarter-elliptical shape were found at the corner. Lengthy fine cracks were observed at the center of the web in a few specimens. The fatigue crack propagation rate in the horizontal direction was high in the early stage of crack propagation but very low in the plate thickness direction when fatigue cracks penetrated near the center of the plate. The relatively fast propagation of cracks in the horizontal direction is due to the coalescing of multiple cracks in this direction. In the direction of the thickness of the plate, cracks start almost simultaneously at the roots of both ends ; in a different plane they independently propagate and overlap near the center of the thickness of the plate, slowing down the propagation rate (Photo 7).

Regardless of any alteration in root gaps or in the depth of welding in HA and HB specimens, there was not much difference in the initiation and propagation behavior of cracks, or in the fatigue strength in different types of specimens. Thus, there is a possibility that fatigue cracks initiate all locations of weld roots in a single-side cruciform joint.

Photo 6 Failure surface of HA₀-1 specimen.Photo 7 Failure surface of HA₀-2 specimen.

4. CONCLUSIONS

Major conclusions from this research are listed below :

- 1) There is not much difference in the fatigue life of various types of fillet welded diaphragm joints tested in study at $R=0$. However, at $R=-1$, fatigue life of joints, appears to be slightly longer than those at $R \geq 0$.
- 2) In three layer fillet welding, when a welding method which makes the flank angle in the first layer as large as possible is employed, fatigue cracks develop at the weld toe of the second layer. The shape of the weld toe varies greatly depending on the conditions of welding ; there is a possibility that fatigue strength becomes reduced.
- 3) For the fillet weld diaphragm joints the possible order of initiation of fatigue cracks is as follows : (1) the section of overlapped welding at the corners, (2) the welding around the diaphragm at the corner of the scallops, (3) and the terminal points of welding in the middle part of a joint. Based on these results, scallops were made at the corners of the diaphragm in the truss chords of the Honshu-Shikoku bridges. In order to produce clean weld terminals ; two welders started welding from a common weld pool, and terminated in the middle section of the diaphragm.
- 4) The 95 % confidence line for survival for the test results for large size fillet welded joints using an improved welding electrode coincides very well with the design curve for C class joints.
- 5) Fatigue life tends to become longer in cruciform joint specimens when compared to box section and H section specimens which are built similar to actual scale and shape. In actual structures, the welding of the diaphragm is manually carried out in a narrow and inconvenient place ; and corner welding, which tends to produce high residual tensile stress is conducted. Considering these facts, it can be concluded that cruciform joint specimens would not simulate fatigue phenomena of actual structures faithfully. Small scale specimens, which have relatively low residual stress, should exaggerate the above trends.
- 6) The fatigue strength of the single-side fillet weld joint is not much different from that of the two-sided fillet welded joint. However, fatigue cracks always initiate at various points in weld roots in single side joints ; no cracks were found at the welding toe on the other side.

REFERENCES

- 1) JSCE : Fatigue design for Honshu-Shikoku Bridges, 1974 (in Japanese).

- 2) JSCE : The Specifications for Steel Railway Bridges, 1974 (in Japanese).
- 3) JSCE : Honshu-Shikoku Bridge-Authority ; The Specifications for Superstructures, 1977 (in Japanese).
- 4) JSCE : Report on the Steel Superstructure of Honshu-Shikoku Bridges, 1983 (in Japanese).
- 5) Shimokawa, H., Takena, K., Itoh, F. and Miki, C. : Effects of Stress Ratios on the Fatigue Strengths of Cruciform Fillet Welded Joints, Proc. of JSCE, No. 344, 1984.
- 6) Gurney, T. B. : The Influence of thickness on the Fatigue Strength of Welded Joints, BOSS 79 Aug, 1979.
- 7) United Kingdom, Department of Energy : Offshore Installations : Guidance on Design and Construction, Proposed New Fatigue Design Rules for Steel Welded Joints in offshore Structures, May 1982.
- 8) Ohta, A., Sasaki, E. and Kosuga, K. : Effect of Stress Ratios on the Fatigue Crack Propagation Rate, Trans. of JSME, Vol. 43, No. 373, pp. 3173~3179, 1977 (in Japanese).
- 9) Maddox S. J. : Assessing the Significance of Flaws in Welds Subject to Fatigue, Metal Construction Sept. 1974.
- 10) Miki, C., Nishimura, T., Tanabe, H. and Nishikawa, K. : Study on Estimation of Fatigue Strengths of Notched Steel Members, Proc. of JSCE, No. 316, pp. 153~166, Dec. 1981.

(Received November 13 1985)
